Ligand Binding Affinity and Changes in the Lateral Diffusion of Receptor for Advanced Glycation Endproducts (RAGE)

Aleem Syed[1], Qiaochu Zhu[1] and Emily A. Smith*

Department of Chemistry, Iowa State University, 1605 Gilman Hall, Ames, IA 50010

*esmith1@iastate.edu, (+1) 515-294-1424 (P), (+1) 515-294-0105 (F)

[1] These authors have contributed equally to the work.

Abstract

The effect of ligand on the lateral diffusion of receptor for advanced glycation endproducts (RAGE), a receptor involved in numerous pathological conditions, remains unknown. Single particle tracking experiments that use quantum dots specifically bound to hemagglutinin (HA)-tagged RAGE (HA-RAGE) are reported to elucidate the effect of ligand binding on HA-RAGE diffusion in GM07373 cell membranes. The ligand used in these studies is methylglyoxal modified-bovine serum albumin (MGO-BSA) containing advanced glycation end product modifications. The binding affinity between soluble RAGE and MGO-BSA increases by 1.8 to 9.7-fold as the percent primary amine modification increases from 24 to 74% and with increasing negative charge on the MGO-BSA. Ligand incubation affects the HA-RAGE diffusion coefficient, the radius of confined domains of diffusion, and duration in confined domains of diffusion. There is, however, no correlation between MGO-BSA ligand binding affinity and the extent of the changes in HA-RAGE lateral diffusion. The ligand induced changes to HA-RAGE lateral diffusion do not occur when cholesterol is depleted from the cell membrane, indicating the mechanism for ligand-induced changes to HA-RAGE diffusion is cholesterol dependent. The results presented here serve as a first step in unraveling how ligand influences RAGE lateral diffusion.

Keywords

Single particle tracking

Membrane biophysics

Fluorescence microscopy

Cholesterol depletion

Receptor signaling

Abbreviations

ERK	Extracellular signal-regulated kinases
HA tag	Hemagglutinin tag
MGO	Methylglyoxal
QDs	Quantum dots
SPT	Single particle tracking

1. Introduction

The receptor for advanced glycation endproducts (RAGE) is a transmembrane receptor that is involved in several pathological disorders [1-3]. It is a multi-ligand pattern-recognition receptor with a diverse array of chemically distinct ligands [4]. Although ligand induced RAGE signaling has been studied extensively in various pathological states, knowledge of the molecular diffusion of RAGE in the cell membrane is generally unknown. The lateral diffusion of membrane proteins plays a role in how receptors interface with other membrane proteins, extracellular ligands, and intracellular proteins, and more generally, how receptors function. The goal of the work reported herein is to understand the effect of ligand incubation on the lateral diffusion and signaling of RAGE in GM07373 bovine artery endothelial cell membranes.

RAGE consists of one variable (V) and two constant (C1 and C2) domains in the extracellular region, a single transmembrane domain and a short cytoplasmic tail. The RAGE extracellular ligand binding domains belong to the immunoglobulin superfamily. RAGE interacts with several ligands including advanced glycation endproducts (AGE), members of the S100/calgranulins family of proteins and amyloid-beta peptides [5-7]. AGE include non-enzymatic modifications of surface amino acid residues lysine, arginine and cysteine, which may lead to protein cross linking. The resulting AGE-modified proteins have a net increase in negative surface charge [8]. Although RAGE ligands are structurally different, all ligands are reported to contain negatively charged regions that are important for binding. Structural analysis of the RAGE extracellular domain with X-ray crystallography and nuclear magnetic resonance spectroscopy corroborates the notion that negatively charged ligands interact with positively charged surfaces of the V and C1-type RAGE ectodomains [9, 10]. The binding between RAGE and its ligands has been measured by several techniques including surface plasmon resonance

(SPR) and ELISA. For example, the dissociation constants measured by SPR with human RAGE were 360 nM and 1.3 μM for glceraldehyde-derived and glycoladehyde-derived AGE, respectively [11]. A SPR analysis of the S100B-soluble RAGE interaction revealed a moderate affinity with an 8.3 μM dissociation constant [12]. Methylglyoxal modified-bovine serum albumin (MGO-BSA, a model AGE similar to the one used herein), binds to the V domain of RAGE with an 800 nM dissociation constant as measured by ELISA [13].

We have recently reported properties of RAGE lateral diffusion as measured by fluorescence recovery photobleaching (FRAP) [14]. The lateral diffusion of RAGE and RAGE-dependent signaling were found to be connected to the dynamics of the actin cytoskeleton. In a FRAP experiment, the measured diffusion parameters represent an ensemble average of numerous receptors. However, receptor lateral diffusion is generally not synchronized across each receptor, and the heterogeneity of all possible diffusion behaviors is not measured by FRAP. For this purpose, it is necessary to probe the diffusion one receptor at a time. One such approach is single particle tracking (SPT), where the receptor is exogenously labeled with a fluorophore and the diffusion of labeled receptor is extracted by following the trajectory of the label [15]. SPT has been used to study the diffusion of a variety of receptors such as G protein-coupled receptors, epidermal growth factor receptor, and homomeric α3-containing glycine receptor [16-18]. For SPT, it is imperative that the signal from the fluorophore be bright and photostable to facilitate fast acquisition times over long durations. Inorganic quantum dots (QDs) satisfy the requirements, and the size of the QD can be of similar magnitude to many receptors. Labeling specificity to the desired receptor is achieved by modifying the QD surface with a ligand or another similar strategy [19]. A recent review article summarizes the use of SPT to measure receptor diffusion [20].

Given the importance of electrostatic interactions in RAGE binding to ligand, increasing the negative charge of the ligand may influence binding and the functional consequences of binding to RAGE; this may include influencing the lateral diffusion of RAGE. To test this hypothesis, MGO-BSA with different extents of primary amine modification are prepared. The extent of modification is characterized by measuring free primary amine content and zeta potentials. Ligand binding between MGO-BSA and soluble RAGE (sRAGE, containing the RAGE extracellular domains V, C1 and C2) is measured *in vitro* using SPR. The effect of ligand on the lateral diffusion of HA-RAGE is measured with single particle tracking (SPT). The role of cholesterol in ligand-induced changes to HA-RAGE lateral diffusion is measured by depleting cellular cholesterol concentrations with methyl-β-cyclodextrin. Finally, ERK phosphorylation is studied in cells to identify possible correlations in HA-RAGE lateral diffusion, signaling, and ligand binding properties.

2. Materials and Methods

2.1. Cell culture, protein expression and Western blotting

All microscopy and molecular biology experiments were performed using bovine artery GM07373 endothelial cells (Coriell Institute Biorepositories, Camden, NJ) maintained according to the procedure described previously [14]. GM07373 cells were transfected with purified recombinant plasmid using Lipofectamine 2000 and the manufacturer's instructions (Life Technology). Transfected GM07373 cells were selected using Geneticin sulfate (Santa Cruz Biotechnology, Inc., Santa Cruz, CA). The transfected cells were established to express HA-RAGE protein stably before microscopy or molecular biology experiments. Details of the HA-

RAGE expression plasmid, soluble RAGE expression and purification and Western blotting experiments are provided in the supplementary material.

2.2. Preparation and characterization of methylglyoxal (MGO) modified-bovine serum albumin (BSA)

BSA was modified with different concentrations of MGO to generate various MGO-BSA. 10 mM, 40 mM, 60 mM, 80 mM and 100 mM MGO was incubated with 50 mg/mL BSA in 0.1 M phosphate buffered saline (PBS) pH 7.4 at 37 °C for five days. On the fifth day, unreacted MGO was removed by dialysis in 0.1 M PBS. The ortho-phthaldialdehyde assay was performed to evaluate the extent of modification *via* quantifying the free primary amine content of BSA [21]. The fluorescence intensity was measured with a microplate reader (Synergy 2 Multi-Mode Reader, BioTek) at excitation and emission wavelengths of 340 nm and 435 nm, respectively. The resulting fluorescence intensities were translated into a percent modification using the signal measured from unmodified BSA (without MGO incubation) as a control.

2.3. Zeta potential measurement

The zeta potential and protein mobility of the prepared MGO-BSA were obtained using a Zetasizer Nano ZS (Malvern Instruments, Ltd) with laser Doppler velocimetry. MGO-BSA and BSA control were diluted five times in PBS solution at pH=7.4. Three replicates were measured for each sample at 25 °C and 200 continuous runs.

2.4. Surface plasmon resonance (SPR)

The binding affinity between MGO-BSA and sRAGE was measured using a home-built SPR instrument. The MGO-BSA was immobilized by physisorption on a 50-nm thick gold film. 100 nM sRAGE in HEPES buffer (pH=7.5) was pumped into a flow cell at the flow rate of 0.8 ml/min for one minute, and then the SPR response was monitored for 20 min. After the 20 min association step, the HEPES buffer was flowed for 1 min at the flow rate of 0.8 ml/min, and then the response during the dissociation step was monitored for an additional 20 min. The kinetic parameters for the MGO-BSA/sRAGE interaction were obtained from the resulting sensorgrams as previously reported using the equations provided in the supplementary material [22].

2.5. Quantum dot conjugation and sample preparation for single particle tracking (SPT)

Quantum dots (QDs, ThermoFisher Scientific) conjugated with streptavidin with an approximate diameter of 15 to 20 nm were used as a fluorescent probe in SPT experiments. 5 µL of streptavidin coated QDs in 1 µM borate buffer were added to 21 µL of monoclonal HA-epitope tag antibody conjugated with biotin (ThermoFisher Scientific) in 74 µL of PBS buffer (pH=7.4) and incubated for 2 hours at room temperature. The resulting anti-HA labeled QDs (AHA-QDs) were stored in the refrigerator until use.

Cells were sub cultured onto 8-well Nunc™ Lab-Tek™ chambered glass slide for 24 hours. On the next day, spread cells were incubated with 3% (W/V) BSA in DMEM (BSA-DMEM) medium overnight before imaging experiments to minimize the nonspecific binding. Cells were either used without further treatment or treated with specific MGO-BSA (5 mg/mL in BSA-DMEM) for 1 h. In the case of sequential cholesterol depletion, cells were further treated

with MβCD (5 mM in BSA-DMEM) before labeling with AHA-QDs. For SPT experiments, AHA-QDs were sonicated for 2 h to avoid aggregation of the QDs. The AHA-QDs were diluted to 100 pM in the imaging medium containing 0.1% (W/V) BSA. The low AHA-QD concentration reduces the possibility that two or more QDs are colocalized within the diffraction volume. Cells were incubated with the AHA-QDs for 15 minutes at 37 ºC in the incubator. Cells were then rinsed with imaging medium five times before mounting the sample onto the microscope.

The SPT experiments were performed using a Nikon Eclipse TE2000U microscope (Melville, NY, USA) operating in wide-field, epi-fluorescence mode with a 100× objective and mercury lamp illumination. Filter sets for excitation (425/45 nm) and emission (605/20 nm) were obtained from Omega Optical (XF304-1, Brattleboro, VT, USA). The microscope was housed inside a physiological chamber. All imaging experiments were performed at 36 ± 2 ºC. Fluorescence images were collected using a PhotonMAX 512 EMCCD camera (Princeton Instrument, Trenton, NJ, USA) with a 40 ms camera exposure time and a full-chip (512×512 pixels) field of view for a total of 40 s.

2.6. QD binding specificity, localization, and tracking

The AHA-QD binding specificity was measured using two cell lines: GM07373 cells that do not express HA-RAGE and GM07373 cells that express HA-RAGE. Nonspecific binding was reported as the average number of AHA-QDs in cells lacking HA-RAGE divided by the average number in cells expressing HA-RAGE. The ImageJ particle tracker 2D/3D plug-in implementing the algorithm developed by Sbalzarini and Koumoutsakos was used for detecting QDs,

localization, and tracking [23, 24]. The intrinsic blinking property of the QDs was used to identify single particles and the extracted single particle trajectories that were at least 8 s in duration (i.e., in between blinking events) were further analyzed.

2.7. SPT data analysis

Extracted single particle trajectories were analyzed using APM_GUI (Analyzing Particle Movement with Graphical User Interface), which is a MATLAB-implemented application based on an established algorithm reported by Simson and co-workers [25, 26]. Diffusion coefficients measured for AHA-QDs on GM07373 cells were used as a threshold to select mobile trajectories to account for the non-specific binding. All mobile trajectories were classified either as confined or as non-confined (Brownian) trajectories based on the probability of particle motion being Brownian in a given region. The probability level or the confinement index (L) was calculated for each trajectory to highlight the regions of confined behavior as described previously [26]. The simulated Brownian trajectories for a range of diffusion coefficients were used to estimate the critical confinement index (L_c) and critical confinement time (t_c). These two parameters were used as a threshold to separate Brownian motion from confined motion. In general, the greater the value of L, the greater the tendency for a trajectory to exhibit confined motion. For a given trajectory, a confined diffusion region is defined by the regions where L increases above L_c for a duration of time longer than t_c. Based on the simulation data for Brownian trajectories, the trajectories with $L > 3.16$ for a duration $t_c > 1.95$ s had a 99.93 % likelihood to be in confined motion. For a trajectory classified as confined, the size of the confinement region, the duration of the confinement time, and the diffusion coefficients inside the confined zones and outside the

confined regions were further analyzed. The plot of mean square displacement (MSD) vs time was used to calculate the characteristic diffusion coefficient of a given region [25]. RAGE is reported to oligomerize on the cell surface in the presence of ligand [27-29]. It is not possible to know if a tracked receptor is a monomer or part of an oligomer based on its diffusion coefficient. This is because the diffusion coefficient has a logarithmic dependence on inverse radius, and is thus not particularly sensitive to clustering.

3. Results and Discussion

3.1. Characterization of MGO-BSA ligand and its interactions with RAGE

Five MGO-BSA samples were prepared by incubating BSA with 10 to 100 mM MGO. Two of the possible amino acid modifications that occur after MGO incubation are shown in Figure S1. The extent of primary amine modification as measured by the ortho-phthaldialdehyde assay increases linearly ($R^2 = 0.98$) when increasing concentrations of MGO are used for the *in vitro* modification of BSA (Figure 1A). The percent primary amine modification ranges from 24 to 74% compared to control BSA that is not incubated with MGO. BSA that has not been incubated with MGO has a net positive surface charge, but all MGO-BSA samples have a net negative surface charge that increases as the MGO concentration used for the modification of BSA increases (Figure 1B).

RAGE ligands mainly bind to the extracellular V and C1 domains [9, 10], so a soluble variant for RAGE (sRAGE) is commonly used as an antigen for binding affinity studies. Surface plasmon resonance measurements of the dissociation constant (K_d) between each MGO-BSA sample and sRAGE are shown in Figure S2. The K_d values obtained from the SPR curves are

shown in Figure 1C. With increasing percent primary amine modification, the affinity of MGO-BSA for sRAGE increases (i.e., the solution concentration of MGO-BSA required to occupy half of the available binding sites on sRAGE decreases). These affinities are of the same order of mangnitude as previously reported for similar RAGE ligands [13]. Combining the results of the affinity and MGO-BSA surface charge measurements, the affinity between sRAGE and MGO-BSA is linearly dependent ($R^2 = 0.94$) on the net MGO-BSA negative surface charge, which is consistent with an interaction to a positively charged binding pocket on the V-domain of sRAGE.

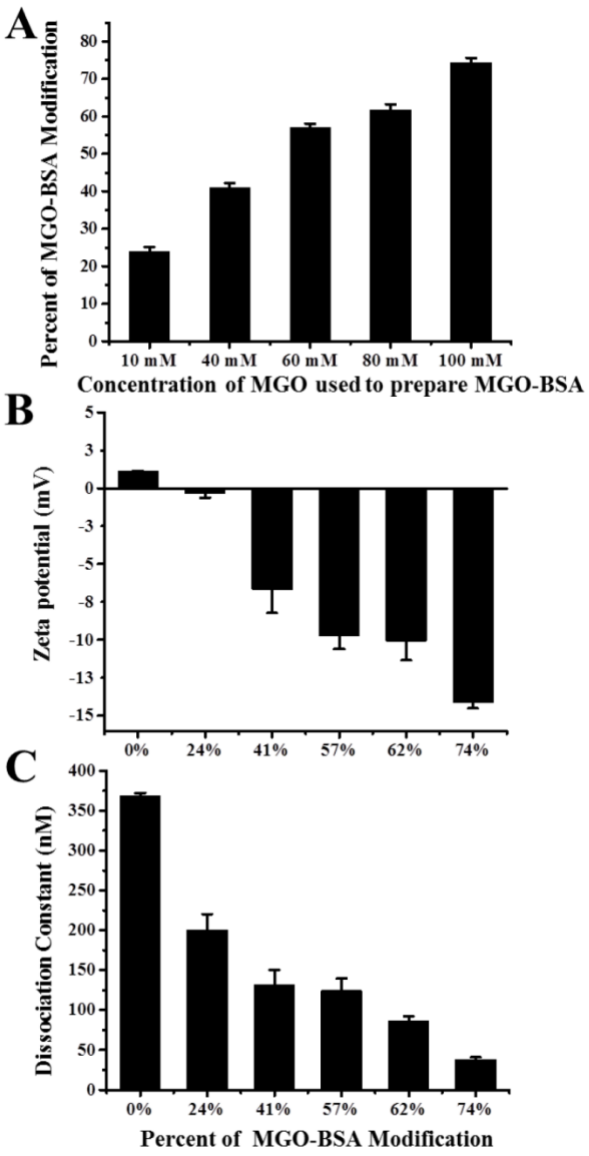

Figure 1. Characterization of methylglyoxal modified-bovine serum albumin (MGO-BSA). (A) Percent modification of free primary amines in BSA as measured by an ortho-phthaldialdehyde assay after modification with the indicated concentration of MGO; (B) Measured Zeta potential for MGO-BSA with the indicated percent primary amine modification; (C) Dissociation constant as measured by SPR for MGO-BSA with the indicated percent primary amine modification and sRAGE.

3.2. Extracellular HA epitope tag enables the specific labeling of QDs to RAGE

Single particle tracking experiments require the specific binding between a nanoparticle and a receptor. In these studies the nanoparticles are fluorescent quantum dots (QDs). A ligand can be directly coated on the surface of the QDs [30, 31], however, up to 88% nonspecific binding is observed when ligand (AGE or S100A8/A9)-coated QDs are incubated with cells that do not express RAGE (data not shown). A possible reason for the observed nonspecific binding may be due to the affinity of RAGE ligands for other membrane proteins [8]. As an alternative specific labeling route, the 9 amino acid (YPYDVPDYA) hemagglutinin (HA) tag was added to the RAGE extracellular domain at a position three amino acids away from the N-terminus of the signal peptide. The cellular signaling in HA-RAGE is similar to RAGE lacking the HA tag as measured by phosphorylation of ERK (p-ERK). There is a two-fold increase in p-ERK in GM07373 cells expressing HA-RAGE compared to GM07373 cells that do not express detectable amounts of RAGE (Figure S3). This increase is consistent with the two-fold increase in p-ERK in GM07373 cells expressing RAGE lacking the HA tag, as reported previously [14]. In addition, a control experiment showed no change in p-ERK when HA-RAGE expressing cells were first exposed to HA antibody, to check for a blocked ligand binding site, followed by incubation with MGO-BSA with 41% primary amine modification (Figure S4).

Anti-HA-coated QDs (AHA-QDs) are generated by incubating streptavidin-coated QDs with biotin-labeled anti-HA to specifically label HA-RAGE. The specific binding of AHA-QDs for HA-RAGE is measured using cells that are incubated with 100 pM AHA-QDs as shown in Figure S5. The number of AHA-QDs per cell is counted for at least 34 cells expressing HA-RAGE or lacking HA-RAGE. There is 4.8% nonspecific AHA-QD binding, indicating that a majority of the AHA-QDs observed in the HA-RAGE expressing cells are specifically bound to

HA-RAGE. A goal of this work is to measure the diffusion properties of HA-RAGE as measured by the trajectories of AHA-QDs. The nonspecifically bound AHA-QDs on the cell membrane are immobile and do not diffuse. To prevent biasing the HA-RAGE diffusion measurements, the immobile AHA-QDs are excluded from the analysis since immobile trajectories could arise from either nonspecific binding or immobile HA-RAGE. Excluding the immobile AHA-QDs from the analysis does prohibit measuring the fraction of immobile HA-RAGE.

3.3. Diffusion properties for the Brownian trajectories of HA-RAGE in the presence and absence of MGO-BSA ligand

Fluorescence microscopy is used to collect at least 400 trajectories of AHA-QDs from at least 10 cells to measure the diffusion of HA-RAGE in the presence or absence of MGO-BSA. Trajectories are classified as exhibiting either Brownian or confined diffusion. If the trajectory has a minimum of one confined domain (where the confinement index (L) is higher than the critical confinement value for longer than the critical time as described in the experimental section) then the trajectory is classified as confined. In the absence of ligand, 31% of HA-RAGE exhibit Brownian diffusion and 69% exhibit confined diffusion, indicating a majority of HA-RAGE measured by SPT exhibit confined diffusion at least once in ~20 seconds (i.e., the average length of a trajectory as shown in Table 1). When the cells are incubated with MGO-BSA, a 3 to 7% increase in the Brownian population is measured when the MGO-BSA percent primary amine modification is at least 41%.

Table 1. Average diffusion parameters for the **Brownian trajectories** of HA-RAGE in the GM07373 cell membrane treated with MGO-BSA with the indicated percent primary amine modification.

	% of Brownian trajectories	**D ($\mu m^2/s$)**	**Average length of the trajectory (s)**
No treatment	31%	0.085	20 ± 10
24% MGO-BSA treatment	31%	**0.039 ($p < 0.01$)**	19 ± 9
41% MGO-BSA treatment	36%	**0.052 ($p < 0.01$)**	19 ± 9
57% MGO-BSA treatment	34%	**0.069 ($p < 0.01$)**	20 ± 10
62% MGO-BSA treatment	39%	**0.115 ($p < 0.01$)**	20 ± 9
74% MGO-BSA treatment	36%	**0.050 ($p < 0.01$)**	30 ± 10

Diffusion coefficients with a p-value below 0.05 are highlighted in bold to show statistically significant differences compared to the cells that were not treated. The percentage of Brownian trajectories is obtained from counting, so no uncertainty is provided.

The average diffusion coefficient for the Brownian trajectories of HA-RAGE in the absence of ligand is 0.085 $\mu m^2/s$. The histogram of diffusion coefficients (Figure 2) shows a bimodal population with maximum diffusion coefficients of 0.0006 and 0.065 $\mu m^2/s$. When the cells are exposed to 24% MGO-BSA, the average diffusion coefficient drops to 0.039 $\mu m^2/s$ (Table 1). The distribution of diffusion coefficients remains bimodal but with a higher percentage of the slower population (Figure 2). Between 24% MGO-BSA and 62% MGO-BSA treatment, there is an increase in the average diffusion coefficient and a decrease in the

population of HA-RAGE in the slower diffusion coefficient range. Interestingly, compared to the 62% MGO-BSA treatments, the average diffusion coefficient decreases after 74% MGO-BSA treatment, and there is a recurrence of the bimodal diffusion coefficient distribution. With increasing percent primary amine modification, the viscosity of the ligand solution increases, which is indicative of protein cross linking. It is possible that the decrease in the diffusion coefficient in going from the 62% to the 74% MGO-BSA sample is a result of extensive protein cross linking. The *in vitro* sRAGE binding studies (i.e., the SPR studies) may be less sensitive to the degree of protein cross linking, possibly because the sRAGE is immobilized in a range of orientations on the sensor surface that may have different binding capacities, while RAGE in the membrane is expected to have fewer degrees of freedom. Thus the affinity measured by SPR may not be representative of the binding affinity of full length RAGE in the cell membrane if extensive protein cross linking is present. It is also possible that ligand binding to another receptor (as stated above AGE binds to other receptors) may indirectly impact RAGE diffusion.

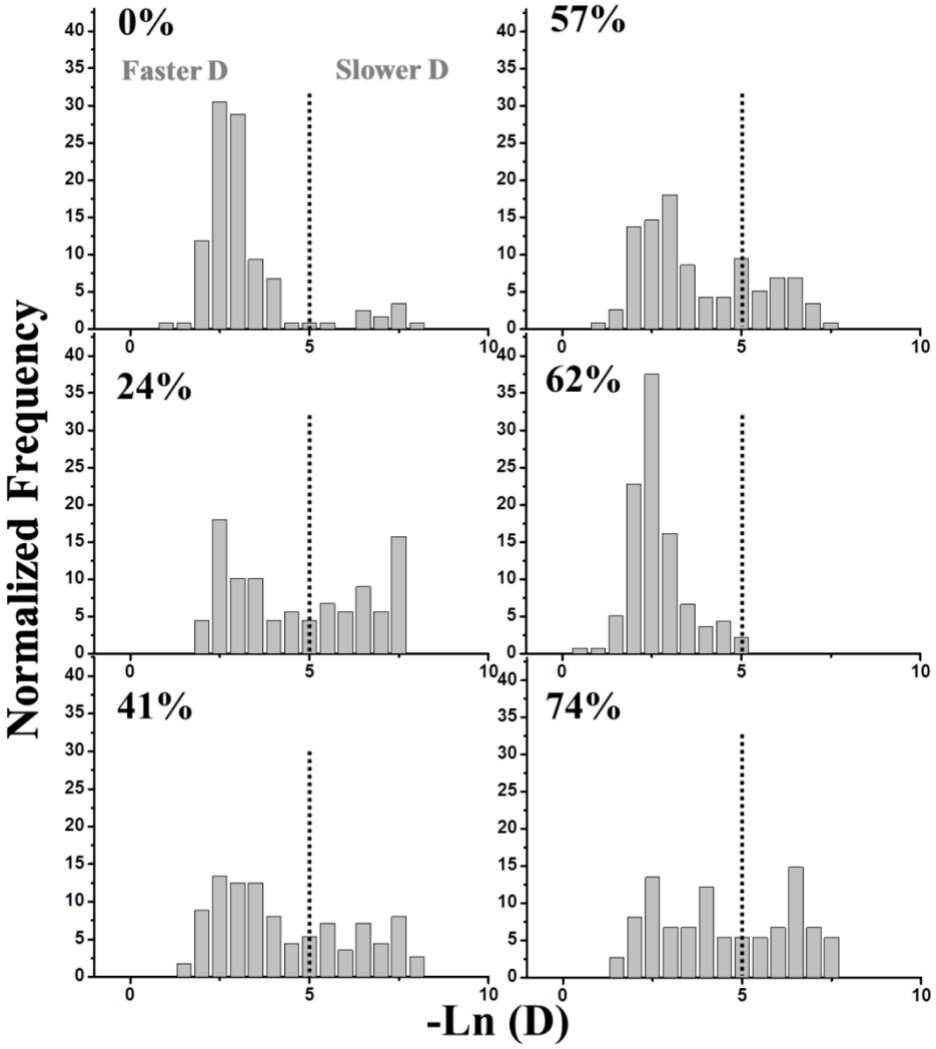

Figure 2. Histograms of diffusion coefficients for the **Brownian trajectories** of HA-RAGE in the GM07373 cell membrane treated with MGO-BSA having the indicated percent primary amine modification. The diffusion coefficient is plotted as the negative natural logarithm; slower diffusion coefficients appear on the right side of the graph. The dotted line is shown for clarity in comparing the changes in the distribution.

3.4. Diffusion properties for the fraction of HA-RAGE with at least one confined domain in the presence and absence of MGO-BSA ligand

Two regions are identified for each trajectory classified as exhibiting a confined domain based on the measured confinement index (L). First, regions inside the confined regions where L is higher than the critical confinement value for longer than the critical time. Second, since the time HA-RAGE is in confined domains (Table 2) is less than the average trajectory time, parts of the trajectory represent diffusion outside confined domains.

Table 2. Average diffusion parameters for the **confined trajectories** of HA-RAGE in the GM07373 cell membrane treated with MGO-BSA with the indicated percent primary amine modification.

	D ($\mu m^2/s$) (Outside confined domains)	**D ($\mu m^2/s$) (Inside confined domains)**	**Radius (μm)**	**Confinement time (s)**	**Average length of the trajectory (s)**
No treatment	0.060	0.012	0.199	3.89	32 ± 9
24% MGO-BSA treatment	**0.031 (p < 0.01)**	**0.007 (p < 0.01)**	**0.138 (p < 0.01)**	**4.09 (p < 0.01)**	31 ± 9
41% MGO-BSA treatment	**0.050 (p < 0.01)**	0.013 (p=0.09)	**0.192 (p < 0.01)**	3.90 (p=0.07)	30 ± 10
57% MGO-BSA treatment	**0.053 (p < 0.01)**	0.011 (p=0.09)	0.195 (p=0.06)	3.99 (p=0.2)	30 ± 10
62% MGO-BSA treatment	**0.085 (p < 0.01)**	**0.026 (p < 0.01)**	**0.294 (p < 0.01)**	3.46 (p=0.19)	31 ± 9
74% MGO-BSA treatment	**0.042 (p < 0.01)**	**0.010 (p=0.01)**	**0.178 (p=0.02)**	**3.97 (p < 0.01)**	20 ± 10

Entries with a p-value below 0.05 are highlighted in bold to show statistically significant differences compared to the cells that were not treated.

Outside of the confined domains, Brownian diffusion properties are expected. Table 2 and Figure 3 confirm that the diffusion coefficients measured outside the confined domains of diffusion are within expected experimental uncertainties to the values measured for the trajectories exhibiting pure Brownian diffusion shown in Table 1 and Figure 2, including a maximum average diffusion coefficient (0.085 $\mu m^2/s$) measured after treatment with 62% MGO-BSA. When HA-RAGE is in a confined domain and in the absence of ligand, the average diffusion coefficient is 7-fold slower compared to HA-RAGE exhibiting Brownian diffusion. For HA-RAGE in confined domains in the presence of MGO-BSA, the same trends are measured in the average diffusion coefficient and the histogram of diffusion coefficients as measured for HA-RAGE exhibiting Brownian diffusion, although the magnitude of the average diffusion coefficient is 4 to 6-fold slower within the confined domains (Table 2 and Figure 4).

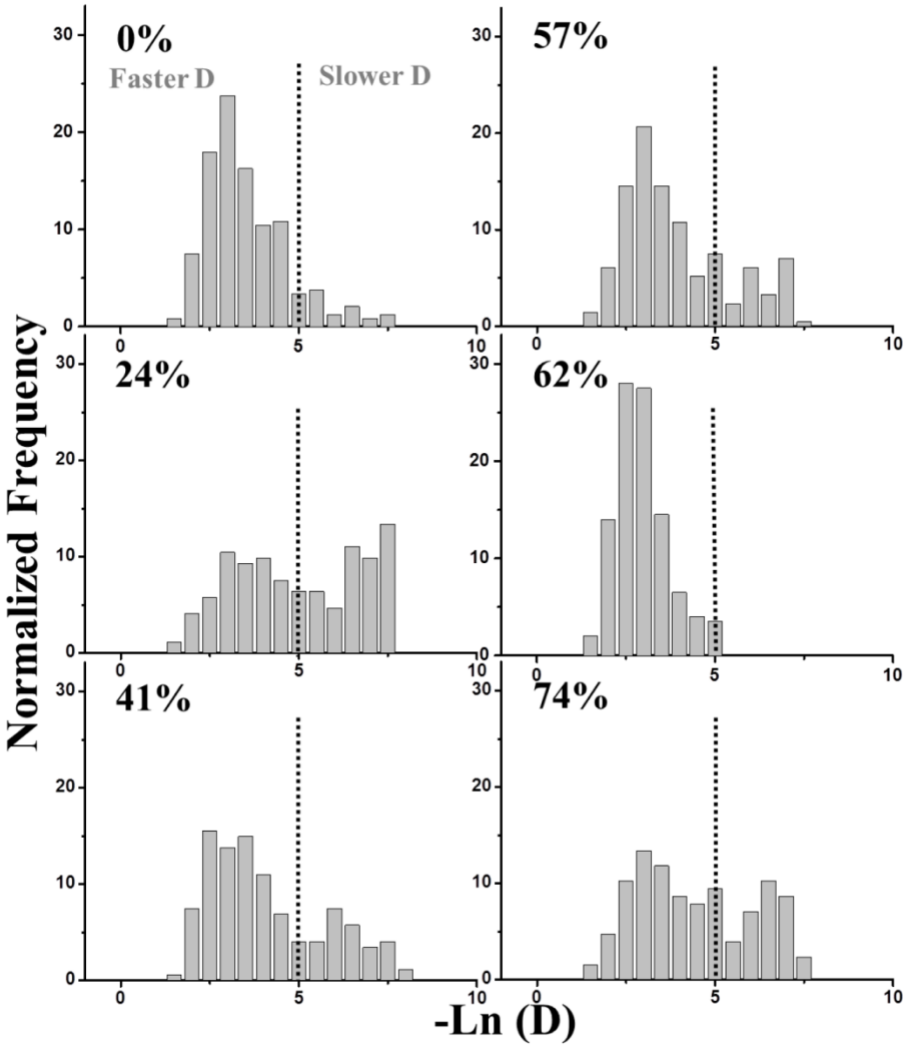

Figure 3. Histograms of diffusion coefficients for the **confined trajectories (outside domains of confined diffusion)** of HA-RAGE in the GM07373 cell membrane treated with MGO-BSA having the indicated percent primary amine modification. The diffusion coefficient is plotted as the negative natural logarithm. The dotted line is shown for clarity in comparing the changes in the distribution.

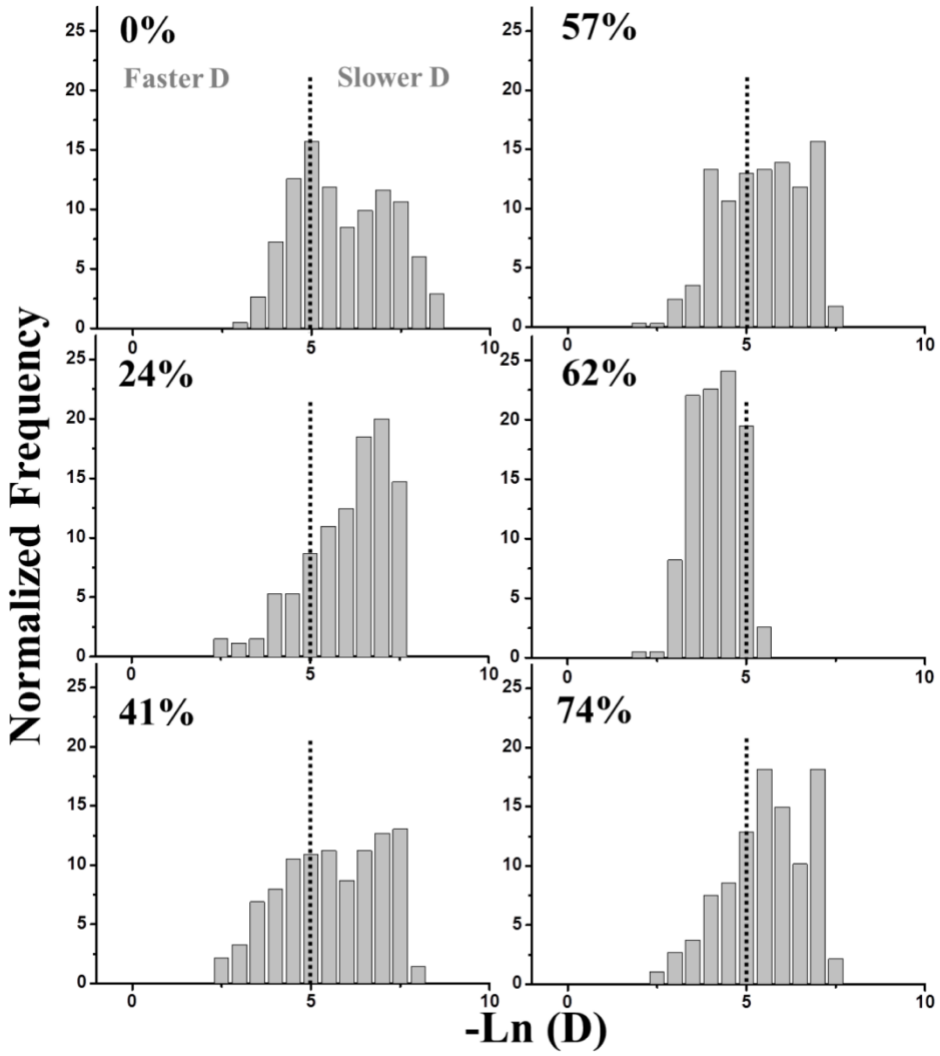

Figure 4. Histograms of diffusion coefficients for the **confined trajectories (inside domains of confined diffusion)** of HA-RAGE in GM07373 cell membrane treated with MGO-BSA having the indicated percent primary amine modification. The diffusion coefficient is plotted as the negative natural logarithm. The dotted line is shown for clarity in comparing the changes in the distribution.

The average confinement radius and time in confined domains measured for HA-RAGE in the absence of ligand were 0.199 μm and 3.89 seconds, respectively (Table 2). The confinement radius decreases after treatment with 24% MGO-BSA, and the confinement radius is the largest after 62% MGO-BSA treatment (Figure 5, Table 2).

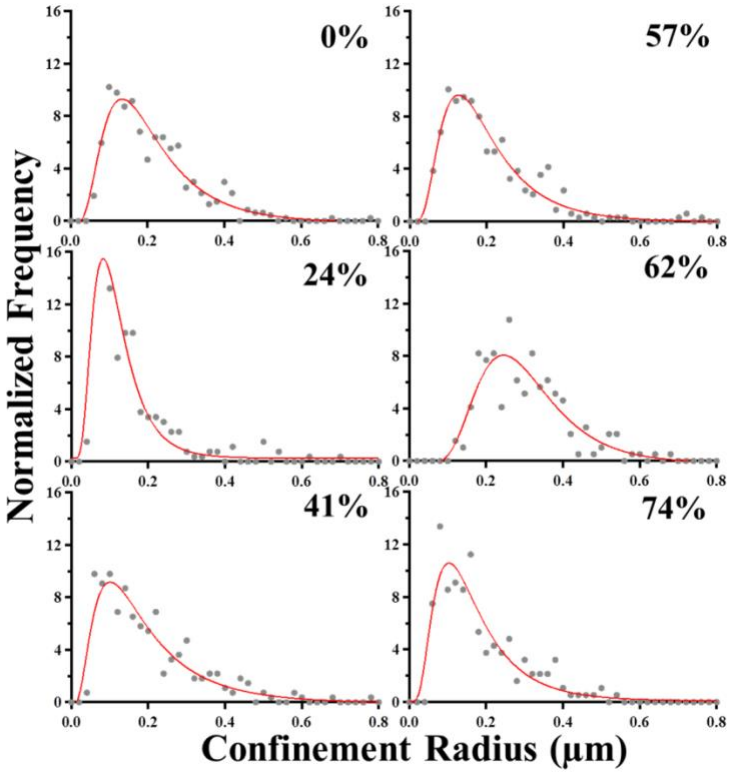

Figure 5. Distribution of confinement radius for the **confined trajectories (inside domains of confined diffusion)** of HA-RAGE in the GM07373 cell membrane treated with MGO-BSA having the indicated percent primary amine modification. The corresponding fits (red solid line) are obtained by fitting the distribution to a log-normal function.

Overall the confinement radius shows the same trend as the average diffusion coefficient with increasing MGO-BSA percent primary amine modification. The time HA-RAGE remains in confined domains remains approximately 4 seconds after cellular incubation with MGO-BSA. While the size of the domains of confined diffusion varies with MGO-BSA incubation, the time HA-RAGE spends within these domains is relatively independent of ligand incubation.

3.5. p-ERK and HA-RAGE expression are independent of the percent primary amine modification on MGO-BSA

Phosphorylation of ERK (p-ERK) and Akt (p-Akt) have been used to measure RAGE signaling [14, 29]. After incubation with MGO-BSA, there is a 2 to 2.4-fold increase in p-ERK compared to p-ERK measured in the absence of MGO-BSA (Figure 6A and 6B). There is no statistically significant difference in p-ERK phosphorylation for cells incubated with varying MGO-BSA percent primary amine modifications. A similar trend was measured for cells lacking HA-RAGE expression (Figure S3). Given the similar response in cells that express HA-RAGE and cells lacking HA-RAGE expression, it is possible that a non-RAGE-dependent mechanism is responsible for some or all of the increase in p-ERK after incubation with MGO-BSA. While it cannot be concluded that MGO-BSA incubation results in a RAGE-dependent increase in p-ERK, the experimental design ensures the changes in the diffusion properties discussed above are specific to RAGE, whether or not they are the result of a direct interaction between MGO-BSA and RAGE or an indirect interaction with other membrane components. In contrast to the increasing p-ERK phosphorylation after MGO-BSA incubation, no statistically significant difference in p-Akt is measured is cells expressing or lacking HA-RAGE (Figure S6).

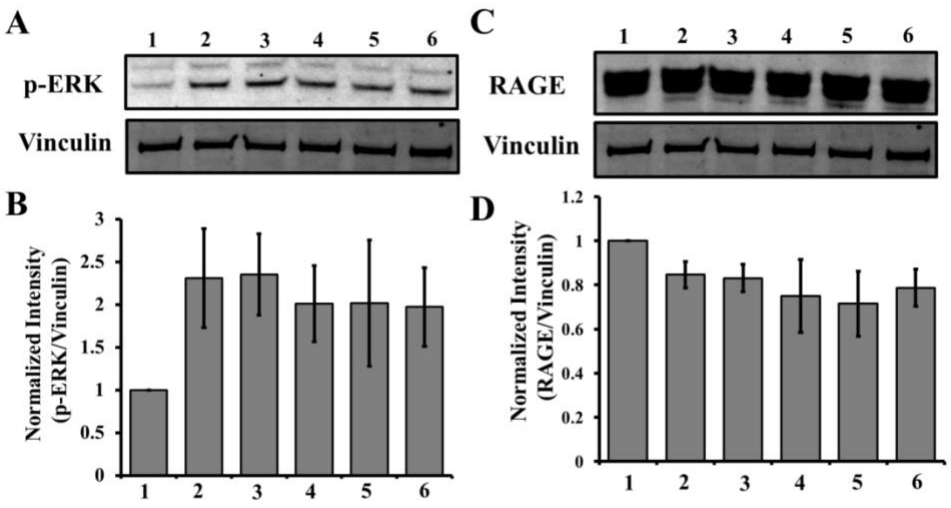

Figure 6. Western blot analysis of phosphorylation of ERK (p-ERK) and HA-RAGE expression in the GM07373 cell lysate with: (Lane 1) no treatment, or 5 mg/mL MGO-BSA treatment with the following percent primary amine modification: (Lane 2) 24%, (Lane 3) 41%, (Lane 4) 57%, (Lane 5) 62%, or (Lane 6) 74%. Fluorescence images of the PVDF membrane probed with: (A) p-ERK antibody or vinculin antibody, and (C) RAGE antibody or vinculin antibody. Average (n = 5) fluorescence intensities of the: (B) 42 kDa band of p-ERK divided by the vinculin band and (D) RAGE band divided by the vinculin band.

There is a 15 to 28% decrease in HA-RAGE expression after incubating cells with MGO-BSA (Figure 6C and 6D). As with p-ERK, the reduced HA-RAGE expression is statistically the same regardless of the percent primary amine modification on MGO-BSA. Previously, RAGE expression was shown to be down regulated in monocytes upon incubation with AGE prepared by glyceraldehyde modification [32]. The glyceraldehyde-prepared AGE reported in this previous study best matches the AGE used in the studies reported herein. In some experimental

conditions, RAGE expression has been shown to be upregulated by incubation with ligand [33, 34].

3.6. Insight into the nature of the confined domains of diffusion: Cholesterol depletion eliminates the ligand-induced changes to HA-RAGE diffusion

Previously RAGE has been reported to be part of cholesterol rich membrane domains [35, 36]. However, cholesterol depletion did not affect the lateral diffusion properties of RAGE as observed with FRAP [14]. As measured by SPT, HA-RAGE diffusion is 2 to 4× slower for Brownian and confined diffusion when cholesterol is extracted from the cell membrane (Table 3, 4). In addition the radius of confined diffusion decreases from 0.199 μm to 0.160 μm after cholesterol extraction. These changes are similar to the changes measured after 24% MGO-BSA incubation (Table 1, 2).

The effect of cholesterol depletion on ligand-induced changes in HA-RAGE lateral diffusion is explored by depleting cholesterol from untreated and 62% MGO-BSA-treated cells. Considering all diffusion properties for Brownian and confined diffusion, the changes in HA-RAGE diffusion that are measured after 62% MGO-BSA treatment are not measured when cholesterol is extracted from the membrane (Table 3, 4 and Figure S7, S8, S9 and S10). After treatment with 62% MGO-BSA and cholesterol extraction, the HA-RAGE diffusion parameters are similar to the values measured after cholesterol extraction without ligand incubation. The 62% MGO-BSA-induced changes in HA-RAGE diffusion are cholesterol dependent, and are not measured when cholesterol concentrations and/or cholesterol-dependent structures in the

membrane are altered. It is possible that the effect of cholesterol depletion on RAGE diffusion is dependent upon the level of primary amine modifications, and is worthy of further study.

Table 3. Average diffusion parameters for the **Brownian trajectories** for HA-RAGE in the GM07373 cell membrane for the indicated cellular treatments.

	% of Brownian trajectories	**D ($\mu m^2/s$)**	**Average length of the trajectory (s)**
No treatment	31%	0.085	20 ± 10
62% MGO-BSA ligand	36%	**0.115 ($p < 0.01$)**	20 ± 9
5 mM MβCD to extract cholesterol	33%	**0.036 ($p < 0.01$)**	19 ± 9
62% MGO-BSA and 5mM MβCD	34%	**0.041 ($p < 0.01$)**	18 ± 9

Diffusion coefficients with a p-value below 0.05 are highlighted in bold to show statistically significant differences compared to the cells that were not treated. The percentage of Brownian trajectories is obtained from counting, so no uncertainty is provided.

Table 4. Average diffusion parameters for the **confined trajectories** for HA-RAGE in the GM07373 cell membrane for the indicated cellular treatments.

	D ($\mu m^2/s$) (Outside confined domains)	**D ($\mu m^2/s$) (Inside confined domains)**	**Radius (μm)**	**Confinement time (s)**	**Average length of the trajectory (s)**
No treatment	0.06	0.012	0.199	3.89	32 ± 9
62% MGO-BSA ligand	**0.085 ($p < 0.01$)**	**0.026 ($p < 0.01$)**	**0.294 ($p < 0.01$)**	3.46 ($p=0.19$)	31 ± 9
5 mM MβCD to extract cholesterol	**0.035 ($p < 0.01$)**	**0.003 ($p < 0.01$)**	**0.160 ($p < 0.01$)**	3.94 ($p=0.55$)	30 ± 10
62% MGO-BSA and 5mM MβCD	**0.038 ($p < 0.01$)**	**0.008 ($p < 0.01$)**	**0.164 ($p < 0.01$)**	3.92 ($p=0.33$)	30 ± 10

Entries with a p-value below 0.05 are highlighted in bold to show statistically significant differences compared to the cells that were not treated.

4. Conclusions

MGO-BSA binding affinity to sRAGE was observed to be dependent on the percent primary amine modification and the net negative surface charge on the ligand. MGO-BSA incubation affected HA-RAGE lateral diffusion, however, there was no direct correlation measured between ligand binding affinity, net negative surface charge on the ligand and HA-RAGE diffusion coefficient, radius of confinement or duration of confinement. This may be the result of increasing levels of protein cross linking with increasing primary amine modification. Cholesterol depletion was found to ameliorate the 62% MGO-BSA ligand induced changes on HA-RAGE lateral diffusion, indicating a direct or indirect role for cholesterol in MGO-BSA-

induced changes to HA-RAGE diffusion. Other factors such as ligand valancy and receptor clustering, as well as, other membrane changes that may result from the MGO-BSA ligand are possible avenues for further study.

5. Acknowledgements

This work was supported by the National Science Foundation (CHE- 1412084). Authors thank Dr. Ann Marie Schmidt (NYU School of Medicine) for providing full length human RAGE plasmid and Dr. Walter Chazin (Vanderbilt University) for providing S100A8/A9 ligand that was tested for preliminary SPT studies and the sRAGE expression system.

6. Conflict of Interest Statement

Authors declare no conflict of interest.

7. References

[1] G.R. Barile, A.M. Schmidt, RAGE and its ligands in retinal disease, Curr Mol Med, 7 (2007) 758-765.
[2] C.D. Logsdon, M.K. Fuentes, E.H. Huang, T. Arumugam, RAGE and RAGE ligands in cancer, Curr Mol Med, 7 (2007) 777-789.
[3] S.D. Yan, X. Chen, J. Fu, M. Chen, H. Zhu, A. Roher, T. Slattery, L. Zhao, M. Nagashima, J. Morser, A. Migheli, P. Nawroth, D. Stern, A.M. Schmidt, RAGE and amyloid-beta peptide neurotoxicity in Alzheimer's disease, Nature, 382 (1996) 685-691.
[4] G. Fritz, RAGE: a single receptor fits multiple ligands, Trends Biochem Sci, 36 (2011) 625-632.
[5] S.D. Yan, A. Bierhaus, P.P. Nawroth, D.M. Stern, RAGE and Alzheimer's disease: a progression factor for amyloid-beta-induced cellular perturbation?, J Alzheimers Dis, 16 (2009) 833-843.
[6] A.M. Schmidt, M. Vianna, M. Gerlach, J. Brett, J. Ryan, J. Kao, C. Esposito, H. Hegarty, W. Hurley, M. Clauss, et al., Isolation and characterization of two binding proteins for advanced glycosylation end products from bovine lung which are present on the endothelial cell surface, J Biol Chem, 267 (1992) 14987-14997.
[7] E. Leclerc, G. Fritz, S.W. Vetter, C.W. Heizmann, Binding of S100 proteins to RAGE: an update, Biochim Biophys Acta, 1793 (2009) 993-1007.
[8] A. Goldin, J.A. Beckman, A.M. Schmidt, M.A. Creager, Advanced glycation end products: sparking the development of diabetic vascular injury, Circulation, 114 (2006) 597-605.
[9] H. Park, F.G. Adsit, J.C. Boyington, The 1.5 A crystal structure of human receptor for advanced glycation endproducts (RAGE) ectodomains reveals unique features determining ligand binding, J Biol Chem, 285 (2010) 40762-40770.
[10] M. Koch, S. Chitayat, B.M. Dattilo, A. Schiefner, J. Diez, W.J. Chazin, G. Fritz, Structural basis for ligand recognition and activation of RAGE, Structure, 18 (2010) 1342-1352.
[11] Y. Yamamoto, H. Yonekura, T. Watanabe, S. Sakurai, H. Li, A. Harashima, K.M. Myint, M. Osawa, A. Takeuchi, M. Takeuchi, H. Yamamoto, Short-chain aldehyde-derived ligands for RAGE and their actions on endothelial cells, Diabetes Research and Clinical Practice, 77 (2007) S30-S40.
[12] T. Ostendorp, E. Leclerc, A. Galichet, M. Koch, N. Demling, B. Weigle, C.W. Heizmann, P.M. Kroneck, G. Fritz, Structural and functional insights into RAGE activation by multimeric S100B, EMBO J, 26 (2007) 3868-3878.
[13] J. Xue, R. Ray, D. Singer, D. Bohme, D.S. Burz, V. Rai, R. Hoffmann, A. Shekhtman, The receptor for advanced glycation end products (RAGE) specifically recognizes methylglyoxal-derived AGEs, Biochemistry, 53 (2014) 3327-3335.
[14] A. Syed, Q. Zhu, E. Smith, Lateral Diffusion and Signaling of Receptor for Advanced Glycation End-products (RAGE): A Receptor Involved in Chronic Inflammation, Eur Biophys J, Submitted (2016).
[15] M.J. Saxton, Single-particle tracking: the distribution of diffusion coefficients, Biophys J, 72 (1997) 1744-1753.
[16] F. Daumas, N. Destainville, C. Millot, A. Lopez, D. Dean, L. Salome, Confined diffusion without fences of a G-protein-coupled receptor as revealed by single particle tracking, Biophys. J., 84 (2003) 356-366.
[17] I. Chung, R. Akita, R. Vandlen, D. Toomre, J. Schlessinger, I. Mellman, Spatial control of EGF receptor activation by reversible dimerization on living cells, Nature, 464 (2010) 783-U163.
[18] K. Notelaers, S. Rocha, R. Paesen, N. Smisdom, B. De Clercq, J.C. Meier, J.M. Rigo, J. Hofkens, M. Ameloot, Analysis of alpha 3 GlyR single particle tracking in the cell membrane, Biochimica Et Biophysica Acta-Molecular Cell Research, 1843 (2014) 544-553.
[19] H. Bannai, S. Levi, C. Schweizer, M. Dahan, A. Triller, Imaging the lateral diffusion of membrane molecules with quantum dots, Nat Protoc, 1 (2006) 2628-2634.
[20] L. Cognet, C. Leduc, B. Lounis, Advances in live-cell single-particle tracking and dynamic super-resolution imaging, Curr Opin Chem Biol, 20 (2014) 78-85.

[21] J.V. Valencia, S.C. Weldon, D. Quinn, G.H. Kiers, J. DeGroot, J.M. TeKoppele, T.E. Hughes, Advanced glycation end product ligands for the receptor for advanced glycation end products: biochemical characterization and formation kinetics, Anal Biochem, 324 (2004) 68-78.
[22] D.J. O'Shannessy, M. Brigham-Burke, K.K. Soneson, P. Hensley, I. Brooks, Determination of rate and equilibrium binding constants for macromolecular interactions using surface plasmon resonance: use of nonlinear least squares analysis methods, Anal Biochem, 212 (1993) 457-468.
[23] I.F. Sbalzarini, P. Koumoutsakos, Feature point tracking and trajectory analysis for video imaging in cell biology, J Struct Biol, 151 (2005) 182-195.
[24] D. Mainali, E.A. Smith, Select cytoplasmic and membrane proteins increase the percentage of immobile integrins but do not affect the average diffusion coefficient of mobile integrins, Anal Bioanal Chem, 405 (2013) 8561-8568.
[25] S.A. Menchon, M.G. Martin, C.G. Dotti, APM_GUI: analyzing particle movement on the cell membrane and determining confinement, BMC Biophys, 5 (2012) 4.
[26] R. Simson, E.D. Sheets, K. Jacobson, Detection of temporary lateral confinement of membrane proteins using single-particle tracking analysis, Biophys J, 69 (1995) 989-993.
[27] J. Xie, S. Reverdatto, A. Frolov, R. Hoffmann, D.S. Burz, A. Shekhtman, Structural basis for pattern recognition by the receptor for advanced glycation end products (RAGE), J Biol Chem, 283 (2008) 27255-27269.
[28] L. Yatime, G.R. Andersen, Structural insights into the oligomerization mode of the human receptor for advanced glycation end-products, FEBS J., 280 (2013) 6556-6568.
[29] H. Zong, A. Madden, M. Ward, M.H. Mooney, C.T. Elliott, A.W. Stitt, Homodimerization Is Essential for the Receptor for Advanced Glycation End Products (RAGE)-mediated Signal Transduction, J. Biol. Chem., 285 (2010) 23137-23146.
[30] X. Michalet, F.F. Pinaud, L.A. Bentolila, J.M. Tsay, S. Doose, J.J. Li, G. Sundaresan, A.M. Wu, S.S. Gambhir, S. Weiss, Quantum dots for live cells, in vivo imaging, and diagnostics, Science, 307 (2005) 538-544.
[31] D. Mainali, E.A. Smith, The effect of ligand affinity on integrins' lateral diffusion in cultured cells, Eur Biophys J, 42 (2013) 281-290.
[32] J. Miura, Y. Uchigata, Y. Yamamoto, M. Takeuchi, S. Sakurai, T. Watanabe, H. Yonekura, S.-i. Yamagishi, Z. Makita, A. Sato, Y. Omori, H. Yamamoto, Y. Iwamoto, AGE down-regulation of monocyte RAGE expression and its association with diabetic complications in type 1 diabetes, Journal of Diabetes and its Complications, 18 (2004) 53-59.
[33] L. Yu, Y. Zhao, S. Xu, F. Ding, C. Jin, G. Fu, S. Weng, Advanced Glycation End Product (AGE)-AGE Receptor (RAGE) System Upregulated Connexin43 Expression in Rat Cardiomyocytes via PKC and Erk MAPK Pathways, International Journal of Molecular Sciences, 14 (2013) 2242-2257.
[34] N. Tanaka, H. Yonekura, S.i. Yamagishi, H. Fujimori, Y. Yamamoto, H. Yamamoto, The Receptor for Advanced Glycation End Products Is Induced by the Glycation Products Themselves and Tumor Necrosis Factor- through Nuclear Factor- B, and by 17 -Estradiol through Sp-1 in Human Vascular Endothelial Cells, J. Biol. Chem., 275 (2000) 25781-25790.
[35] O. Sbai, T.S. Devi, M.A. Melone, F. Feron, M. Khrestchatisky, L.P. Singh, L. Perrone, RAGE-TXNIP axis is required for S100B-promoted Schwann cell migration, fibronectin expression and cytokine secretion, J Cell Sci, 123 (2010) 4332-4339.
[36] M.P. Lisanti, P.E. Scherer, J. Vidugiriene, Z. Tang, A. Hermanowski-Vosatka, Y.H. Tu, R.F. Cook, M. Sargiacomo, Characterization of caveolin-rich membrane domains isolated from an endothelial-rich source: implications for human disease, J Cell Biol, 126 (1994) 111-126.

Graphical Abstract